Further proofs for the 1-photon path Entanglement communications scheme

Remi Cornwall

University of London Alumni Society, Malet Street, London WC1E 7HU
http://webspace.qmul.ac.uk/rocornwall   http://ulondon.academia.edu/RemiCornwall

Abstract
The author had previously set out devices to communicate over space-like intervals, with a full proof for the 2-photon device and only a partial proof for the 1-photon device. The 2-photon device exploits entangled pairs; the 1-photon device utilises path-entanglement. The 1-photon device is fully analysed, then similarities (and differences) are drawn to the 2-photon device to show the holes in the No-communications Theorem: the creation operators representing the sum of paths through the device can be mapped outside the device and quantum state reduction/measurement is a space-like operation. Furthermore, global phase factors indicating causal delay are removed by the trace operation anyway.

Keywords: EPR, Bell's Theorem, Aspect-Zbinden Experiments, No-communications theorem

1. Introduction

Interest in space-like communication has been aroused by the EPR paradox, Bell[1-2], then Aspect, Grangier and Roger's[3], then Gisin and Zbinden's[4] experiments. The correlations that exist are much more than classical correlations (as proven by Bell), as they aren't predetermined and happen at the instant of measurement and appear to be a physical effect, though other interpretations exist[5-7]. Cosmic censorship-type theories[8-10] have been shown wanting by the author– indeed the author has corresponded with the said theoreticians, with one open-minded and the others shutting down the discussion. As regards noted experimenters in the field (such as listed by reference above), a similar situation exists and for the open-minded one, this paper hopes to address their concern regarding the 1-photon setup[11], where they admitted modulation but were doubtful on the information being sent over a space-like separation.

We regard this project as being on a more secure footing for the hard experimental facts-of-the-matter[3-4] with related phenomena *and* the theoretical underpinning killing off the censorship theories[11-13], which show new ground to, perhaps, patch old systems of thought to the new phenomena[14]. This in contrast to experiment lead only claims (as Sagan said, "Extraordinary claims require extraordinary evidence") such as the celebrated 2011 CERN fast neutrino mistake[15], which in that case was down to a delay in a data line. However, this is not to dismiss any marginal, purely experimental claims[16] of superluminal effects, despite the results largely being asserted to be believed (rather than proven by first principles as a contradiction to existing theories or built on

robust well acknowledged phenomena with agreed interpretations).

The author first looked into a 2-photon communication device[13, 17] (figure 1). This used two photons in HV polarisation in one of the Bell states, which were produced by a process of spontaneous parametric down-conversion. The source was in the middle with one photon being sent to "Alice" where she measured or not and the other photon was sent to "Bob's" interferometer. The act of Alice's measurement was discerned by Bob for the production of a mixed state. If she left her photon alone, Bob would perceive interference.

Michael Hall's incredulous initial words (private correspondence) about this were "you don't believe that the state $|H\rangle|V\rangle + |V\rangle|H\rangle$ behaves like $|H\rangle + |V\rangle$ through the interferometer?" His view point, along with Ginacarlo Ghiradi's was that the mere act of looking at one particle in the pair would automatically cause the mixed state, the system wasn't factorisable. However the author found a flaw in the No-communications theorem (NCT): one has to consider the joint evolution[13] of both systems (through space and then the interferometer apparatus) and both acts were unitary; the system stayed entangled even after the interferometer and Bob could discern interference (or not) effects[13]. Interestingly the entanglement of the 2-photons was swapped to path entanglement of one photon of the pair (Bob's) as it went through the interferometer. It became a simple matter to show by state vector reduction or by using the density matrix form, that the collapse process was space-like, that is, there appears to be no dynamics to the process[4] (no wave equation etc.) and all that mattered was the sequence in which the two operations were performed (Alice or Bob measures first).
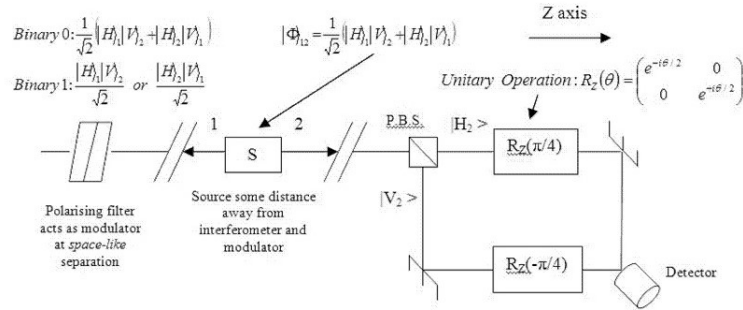
Figure 1 – 2-photon setup

Measurement/Modulation at distant system and state of two photon system	State of distant system	State of local system	Local measurement by interferometer after modulation of distant system
No modulation: 'Binary 0' $\frac{1}{\sqrt{2}}\left(|H\rangle_1|V\rangle_2 + |H\rangle_2|V\rangle_1\right)$	Entangled => Pure state $\frac{1}{\sqrt{2}}\left(|H\rangle_1 + |V\rangle_1\right)$ **Behaves as**, see Appendix1: arxiv.org/abs/1106.2258	Entangled => Pure state $\frac{1}{\sqrt{2}}\left(|V\rangle_2 + |H\rangle_2\right)$ **Behaves as**, see Appendix1: arxiv.org/abs/1106.2258	Pure state results in interference (Or at least some interference since source is not ideally pure)
Modulation: 'Binary 1' $\frac{|H\rangle_1|V\rangle_2}{\sqrt{2}}$ or $\frac{|H\rangle_2|V\rangle_1}{\sqrt{2}}$	Not entangled <=> $\frac{|H\rangle_1}{\sqrt{2}}$ or $\frac{|V\rangle_1}{\sqrt{2}}$ Mixed state	Not entangled <=> $\frac{|H\rangle_2}{\sqrt{2}}$ or $\frac{|V\rangle_2}{\sqrt{2}}$ Mixed state	Mixed state gives no interference

A single photon source (SPS) is incident on a Mach-Zehnder type interferometer with 50:50 beamsplitters. Alice's measurements discerned over space-like separations by Bob at his detectors C (constructive) or D (destructive). Many single photons (a spot from a beam-expander is used with an attenuator on a laser source) are used to represent one bit.
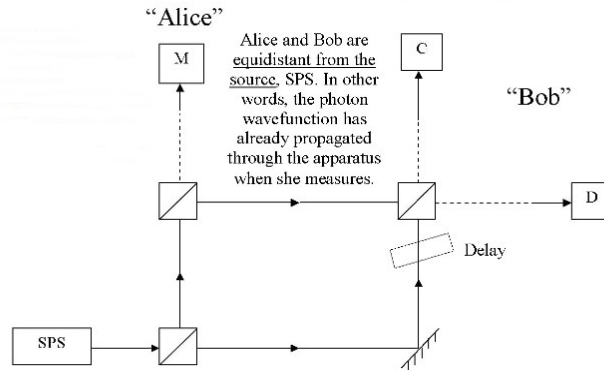

Figure 2 – 1-photon setup

This is the fundamental law of Quantum Mechanics:-

If the paths can be distinguished then add probabilities

else if the paths can't be, then add amplitudes before calculating probabilities

Thus when Alice measures, both of Bob's paths to his detectors become distinguishable.

Alice sends	Bob receives
Binary 0: No measurement	Binary 0: Min signal, destructive interference from pure state at D
Binary 1: Measurement	Binary 1: Max signal from mixed state at D

$$P\left(Bob\ few\ photons,\ binary\ 0\ \ Alice\ no\ measurement\right) = \left|\frac{i}{\sqrt{2}}\right|^2 + \left|\frac{e^{i\theta}}{\sqrt{4}}\right|^2 + 2\left|\frac{i}{\sqrt{2}}\right|\left|\frac{e^{i\theta}}{\sqrt{4}}\right|\cos\theta$$

$$= 0.5 + 0.25 \div \frac{1}{\sqrt{2}}\cos\theta$$

$$\simeq 0.75 \pm 0.707\cos\theta$$

$$\simeq 0.043\ \text{minimum}$$

$$P\left(Bob\ lots\ of\ photons,\ binary\ 1\ \ Alice\ measurement\right) = \left|\frac{i}{\sqrt{2}}\right|^2 + \left|\frac{i}{\sqrt{4}}\right|^2$$

$$= 0.5 + 0.25$$

$$= 0.75$$

Next in the said paper[13] the 1-photon system (figure 2) was re-appraised (originally presented in [11]) and stressed that the result obtained did not speak about sub-systems, tensor products and partial traces but just one particle, with the sum of paths/sum of amplitudes approach; this was seen as a further foil to NCT, which was couched in such terms. Hugo Zbinden pointed out (private correspondence) that the device was correct (as by the sum of paths approach) but he didn't think it would allow space-like communication. He is of course correct – the sum of path proof shows only *modulation* but it doesn't necessarily show space-like communication. This then is the goal of this paper, to complete the proof and show state reduction/collapse by a similar method to the 2-photon considerations.

> The key point to Zbinden's limiting belief was that Alice was close to the interferometer (figure 2) and her influence through measurement, propagated causally through the interferometer to Bob and of course this occurred at the speed of light.

Zbinden's mind-set is limited to the dimensions of the device (although figure 2 implied Alice and Bob were a long way from the interferometer, see figure 3 with its depiction of the wavefunction).
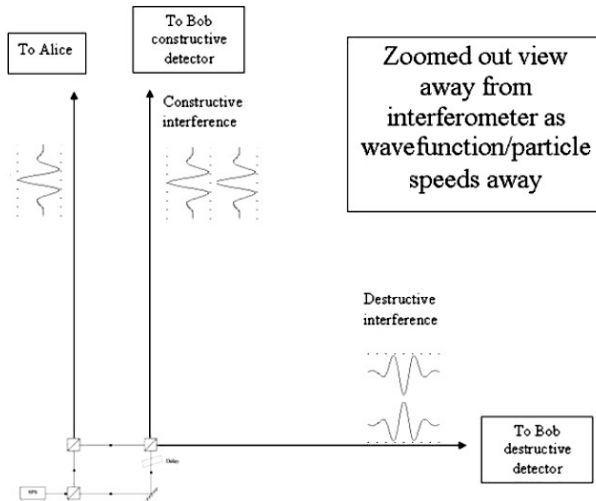

Figure 3 – Alice and Bob at a distance much greater than the dimensions of the device

The proof for the 2-photon setup (figure 1) didn't dwell on the dimensions of the interferometer because it was inferred automatically that both the protagonists were a long way from the source in the centre, which was equidistant from their detectors/modulators. The analysis popped out fine and if state collapse is to be believed[4] deduced space-like communication.

So in a nutshell, to dispel Zbinden's concerns, our final proof for the 1-photon setup only has to show the creation operators at the first beam-splitter (figure 2) mapped outside the device and that there is a sum of upper (modulated by Alice) and lower path wavefunctions. If the implication of the state collapse procedure is correct, distance has no bearing on the matter.

2. Modelling by the state vector approach considering each output as a sub-system

Let us concentrate on the modified MZ interferometer setup and label the inputs and outputs (figure 4). The letters in brackets means that that port is unused. For a 1:1 beamsplitter, the transfer function leads to the rule for mapping the creation operators to the output[18-20] in the Heisenberg evolution picture, thus:

$$\hat{a}^\dagger_{input}\,|0\rangle \rightarrow \frac{1}{\sqrt{2}}\left(\hat{a}^\dagger_{transmitted} + i\hat{a}^\dagger_{reflected}\right)|0\rangle \quad \text{eqn. 1}$$

And so we can model the path of a single photon through the device:

$$\hat{a}^\dagger_a\,|0_h\rangle|0_k\rangle|0_l\rangle$$
$$\rightarrow \frac{1}{\sqrt{2}}\left(\hat{a}^\dagger_c + i\hat{a}^\dagger_d\right)|0_h\rangle|0_k\rangle|0_l\rangle \qquad\qquad \text{eqn. 2}$$
$$\rightarrow \frac{1}{\sqrt{2}}\left(\hat{a}^\dagger_c + \frac{ie^{i\theta_1}}{\sqrt{2}}\left(\hat{a}^\dagger_h + i\hat{a}^\dagger_g\right)\right)|0_h\rangle|0_k\rangle|0_l\rangle$$

The possible output states are shown as a tensor product. An arbitrary phase has been introduced $e^{i\theta_1}$ along the path from *d* to *f*, and the output at *d* becomes the input at *f*, which then is transformed by eqn. 1 to the outputs *h* and *g*.

Continuing in the same vein for output *c*, off the mirror, through the delay to the last splitter and outputs *l* and *k* ($e^{i\theta_2}$), this is obtained,

$$\hat{a}^\dagger_a\,|0\rangle_h|0\rangle_k|0\rangle_l$$
$$\rightarrow \frac{1}{\sqrt{2}}\left(\frac{ie^{i\theta_2}}{\sqrt{2}}\left(\hat{a}^\dagger_l + i\hat{a}^\dagger_k\right) + \frac{ie^{i\theta_1}}{\sqrt{2}}\left(\hat{a}^\dagger_h + i\hat{a}^\dagger_g\right)\right)|0\rangle_h|0\rangle_k|0\rangle_l$$
$$\text{eqn. 3}$$

And once again, finally, to change the output *g* to an input at *i* and then outputs at *l* and *k* (introducing another arbitrary phase $e^{i\theta_3}$ along the leg *g* to *i*. This expression has mapped the creation operators all the way through to the other side of the device:-
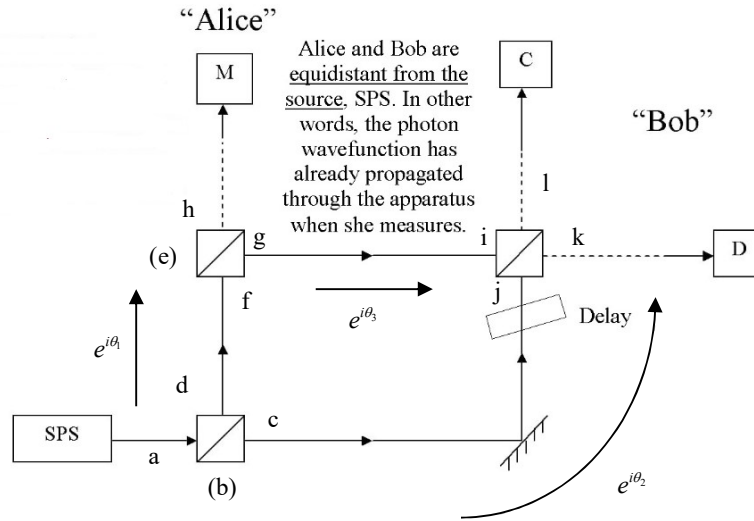
Figure 4 – Ports of the 1-photon device enumerated

$$\hat{a}_a^\dagger |0\rangle_h |0\rangle_k |0\rangle_l$$
$$\rightarrow \frac{1}{\sqrt{2}}\left(\frac{ie^{i\theta_2}}{\sqrt{2}}\left(\hat{a}_l^\dagger + i\hat{a}_k^\dagger\right) + \frac{ie^{i\theta_1}}{\sqrt{2}}\left(\hat{a}_h^\dagger + \frac{ie^{i\theta_3}}{\sqrt{2}}\left(i\hat{a}_l^\dagger + \hat{a}_k^\dagger\right)\right)\right)|0\rangle_h |0\rangle_k |0\rangle_l$$

eqn. 4

Figure 5 – The Creation Operators mapped to the other side of the interferometer

Note that the port k is transmitted and l is reflected in the final expression.

Most people would agree that eqn. 4 is sufficient to show not only the modulation scheme of figure 2 but that it is space-like too – the superimposed wavefunctions it represents coming from the upper and lower paths can be any distance away from the source or device (as shown in figure 3). Netherthless we shall carry the analysis through to the end by the state vector or the density matrix approach.

Tidying up,

$$\hat{a}_a^\dagger |0\rangle_h |0\rangle_k |0\rangle_l \rightarrow \frac{1}{\sqrt{2}}\left(\frac{ie^{i\theta_2}}{\sqrt{2}}\left(\hat{a}_l^\dagger + i\hat{a}_k^\dagger\right) + \frac{ie^{i\theta_1}}{\sqrt{2}}\left(\hat{a}_h^\dagger + \frac{ie^{i\theta_3}}{\sqrt{2}}\left(i\hat{a}_l^\dagger + \hat{a}_k^\dagger\right)\right)\right)|0\rangle_h |0\rangle_k |0\rangle_l$$

$$\rightarrow \left(\frac{ie^{i\theta_1}}{2}\hat{a}_h^\dagger + \frac{i}{2}\left(e^{i\theta_2} - \frac{1}{\sqrt{2}}e^{i(\theta_1+\theta_3)}\right)\hat{a}_l^\dagger - \frac{1}{2}\left(e^{i\theta_2} + \frac{1}{\sqrt{2}}e^{i(\theta_1+\theta_3)}\right)\hat{a}_k^\dagger\right)|0\rangle_h |0\rangle_k |0\rangle_l$$

eqn. 5

Yet more tidying,

$$\hat{a}_a^\dagger |0\rangle_h |0\rangle_k |0\rangle_l \rightarrow \left(\frac{ie^{i\theta_1}}{2}\hat{a}_h^\dagger + \frac{e^{-i\theta_2}}{2}\left[i\left(1 - \frac{1}{\sqrt{2}}e^{i\theta}\right)\hat{a}_l^\dagger - \left(1 + \frac{1}{\sqrt{2}}e^{i\theta}\right)\hat{a}_k^\dagger\right]\right)|0\rangle_h |0\rangle_k |0\rangle_l$$

$$\rightarrow \left(\frac{ie^{i\theta_1}}{2}\hat{a}_h^\dagger + \frac{e^{-i\theta_2}}{2}\left[e^{i\frac{\pi}{2}}\left(1 - \frac{1}{\sqrt{2}}e^{i\theta}\right)\hat{a}_l^\dagger + e^{i\pi}\left(1 + \frac{1}{\sqrt{2}}e^{i\theta}\right)\hat{a}_k^\dagger\right]\right)|0\rangle_h |0\rangle_k |0\rangle_l$$

eqn. 6

The result of the calculation leads to the wavefunction (figure 6) below (which clearly is entangled),

$$|\psi\rangle = \frac{1}{2}|1_h\rangle|0_k\rangle|0_l\rangle + \left(\frac{1}{2} + \frac{1}{2\sqrt{2}}e^{i\theta}\right)|0_h\rangle|1_k\rangle|0_l\rangle + \left(\frac{1}{2} - \frac{1}{2\sqrt{2}}e^{i\theta}\right)|0_h\rangle|0_k\rangle|1_l\rangle$$

eqn. 7

The global phases have been left out, as they make no difference in the expectation values but the path phase difference is shown in the variable θ. The effect of the glass plate delay can be seen at outputs k and l as a favouring of a particular output. The wavefunction moves through space as a superposition of these output states.
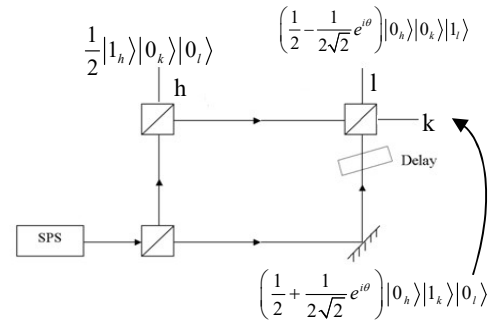

Figure 6 – Unmeasured by Alice case

The act of no measurement by Alice (call it binary 0) gives interference at Bob. The expectation value at Bob's detectors can be found (with the number operator) and tracing out the redundant states, i.e.

Bob's *l* output:

$$\langle 1_l | N^\dagger \left(\frac{1}{2} + \frac{1}{2\sqrt{2}} e^{-i\theta} \right) \left(\frac{1}{2} + \frac{1}{2\sqrt{2}} e^{i\theta} \right) N | 1_l \rangle$$ eqn. 8

$$= \frac{3}{8} + \frac{\cos\theta}{2\sqrt{2}}$$ cf figure 2 with differential output across *l* and *k*

Bob's *k* output:

$$\langle 1_k | N^\dagger \left(\frac{1}{2} - \frac{1}{2\sqrt{2}} e^{-i\theta} \right) \left(\frac{1}{2} - \frac{1}{2\sqrt{2}} e^{i\theta} \right) N | 1_k \rangle$$ eqn. 9

$$= \frac{3}{8} - \frac{\cos\theta}{2\sqrt{2}}$$ cf figure 2 with differential output across *l* and *k*

To illustrate the act of measurement by Alice (binary 1), we could use the approach in the paper "Superluminal Signalling by Path Entanglement"[11], with the state vector approach and manually insert the fact of decoherence at Alice's splitter by her measurement as a random phase. Let us return to eqn. 4 and notice that its form is a sum of paths on the upper and lower legs of figure 2 after the final splitter (hence the forward arrow on the subscripts on the creation operators),

$$\hat{a}_a^\dagger | 0 \rangle_h | 0 \rangle_k | 0 \rangle_l$$

$$\rightarrow \frac{1}{\sqrt{2}} \left(\frac{\frac{PhaseUpper}{\sqrt{2}} \left(\hat{a}_{upper\rightarrow}^\dagger \right)}{+ \frac{PhaseLower}{\sqrt{2}} \left(\hat{a}_{lower\rightarrow}^\dagger \right)} \right) | 0 \rangle_h | 0 \rangle_k | 0 \rangle_l$$ eqn. 10

i.e. $\psi_{output} = \psi_{upper}^{\rightarrow} + \psi_{lower}^{\rightarrow}$

Then the upper phase would be some random function $\theta_{random}(t)$ to render the averaging process of the detectors of the detectors at eqn. 8 and eqn. 9 with no discernable/coherent phase relationship between the two arms on any timescale, such that now the detectors register 3/8 each (so 3/4 in total if a differential output across Bob's detectors is taken, as per figure 2). However, a much more graceful approach is to use the density matrix formalism and then to trace out Alice's subsystem.

3. The Density Matrix approach

We return to the method of eqn. 10 and construct two wavefunctions for the upper and lower paths respectively from eqn. 4 and note:

$$\boxed{\psi_{output} = \psi_{lower}^{\rightarrow} + \psi_{upper}^{\rightarrow}}$$

It is an important point (the reason why the wavefunctions on the RHS have superscripts with arrows) that this is a combination of the upper and lower paths ***after*** they have gone through the beam

splitter. As mentioned earlier, a global phase has no effect on the expectation values and furthermore, this global phase would indicate a causal delay in traversing the beamsplitter but this is irrelevant in state collapse and the expectation values obtained – Quantum Mechanics indicates the process is space-like. This shall be returned to in the conclusion.

The two wavefunctions by eqn. 4 are:

$$\psi_{upper}^{\rightarrow} = \frac{e^{i\left(\theta_1 + \frac{\pi}{2}\right)}}{\sqrt{2}} | 1_h \rangle | 0_k \rangle | 0_l \rangle$$

$$- \frac{e^{i(\theta_1 + \theta_3)}}{2} | 0_h \rangle | 1_k \rangle | 0_l \rangle$$ eqn. 11

$$- \frac{e^{i\left(\theta_1 + \theta_3 + \frac{\pi}{2}\right)}}{2} | 0_h \rangle | 0_k \rangle | 1_l \rangle$$

$$\psi_{lower}^{\rightarrow} = - \frac{e^{i\theta_2}}{2} | 0_h \rangle | 1_k \rangle | 0_l \rangle$$ eqn. 12

$$+ \frac{e^{i\left(\theta_2 + \frac{\pi}{2}\right)}}{2} | 0_h \rangle | 0_k \rangle | 1_l \rangle$$

A moment's thought will have us realise that the whole density matrix isn't just the sum of two matrices,

$$(U_i + L_i) | \psi \rangle \langle \psi | (U_j^* + L_j^*)$$
$$= U_i | \psi \rangle \langle \psi | U_j^*$$
$$+ U_i | \psi \rangle \langle \psi | L_j^* + L_i | \psi \rangle \langle \psi | U_j^*$$ eqn. 13
$$+ L_i | \psi \rangle \langle \psi | L_j^*$$

So,

$$\rho_{hkl} = | \psi \rangle \langle \psi | \quad =$$

	$\langle 0_l | \langle 0_k | \langle 1_h |$	$\langle 0_l | \langle 1_k | \langle 0_h |$	$\langle 1_l | \langle 0_k | \langle 0_h |$
$\lvert 1_h \rangle \lvert 0_k \rangle \lvert 0_l \rangle$	$\frac{e^{i(2\theta_1 + \pi)}}{2}$	$-\frac{e^{i\left(-\theta_3 + \frac{\pi}{2}\right)}}{2\sqrt{2}}$	$-\frac{e^{-i\theta_3}}{2\sqrt{2}}$
$\lvert 0_h \rangle \lvert 1_k \rangle \lvert 0_l \rangle$	$-\frac{e^{i\left(\theta_3 - \frac{\pi}{2}\right)}}{2\sqrt{2}}$	$\frac{e^{i2(\theta_1 + \theta_3)}}{4}$	$\frac{e^{-i\frac{\pi}{2}}}{4}$
$\lvert 0_h \rangle \lvert 0_k \rangle \lvert 1_l \rangle$	$-\frac{e^{i\theta_3}}{2\sqrt{2}}$	$\frac{e^{i\frac{\pi}{2}}}{4}$	$\frac{e^{i(2\theta_1 + 2\theta_3 + \pi)}}{4}$

Upper

	$\langle 0_l | \langle 0_k | \langle 1_h |$	$\langle 0_l | \langle 1_k | \langle 0_h |$	$\langle 1_l | \langle 0_k | \langle 0_h |$
$\lvert 1_h \rangle \lvert 0_k \rangle \lvert 0_l \rangle$	0	0	0
+ $\lvert 0_h \rangle \lvert 1_k \rangle \lvert 0_l \rangle$	0	$\frac{e^{i2\theta_2}}{4}$	$-\frac{e^{-i\frac{\pi}{2}}}{4}$
$\lvert 0_h \rangle \lvert 0_k \rangle \lvert 1_l \rangle$	0	$-\frac{e^{i\frac{\pi}{2}}}{4}$	$\frac{e^{i2\theta_2 + \pi}}{4}$

Lower

$+ \rho_{UL^*} + \rho_{LU^*}$

eqn. 14

With,

$$\rho_{UL^*} =$$

$$\begin{array}{c} \\ |1_h\rangle|0_k\rangle|0_l\rangle \\ |0_h\rangle|1_k\rangle|0_l\rangle \\ |0_h\rangle|0_k\rangle|1_l\rangle \end{array} \begin{array}{ccc} \langle 0_l|\langle 0_k|\langle 1_h| & \langle 0_l|\langle 1_k|\langle 0_h| & \langle 1_l|\langle 0_k|\langle 0_h| \\ \begin{pmatrix} 0 & -\dfrac{e^{i\left(\theta_1-\theta_2+\frac{\pi}{2}\right)}}{2\sqrt{2}} & \dfrac{e^{i(\theta_1-\theta_2)}}{2\sqrt{2}} \\ 0 & \dfrac{e^{i(\theta_1-\theta_2+\theta_3)}}{4} & -\dfrac{e^{i\left(\theta_1-\theta_2+\theta_3-\frac{\pi}{2}\right)}}{4} \\ 0 & \dfrac{e^{i\left(\theta_1-\theta_2+\theta_3+\frac{\pi}{2}\right)}}{4} & -\dfrac{e^{i(\theta_1-\theta_2+\theta_3)}}{4} \end{pmatrix} \end{array}$$

eqn. 15

And,

$$\rho_{LU^*} =$$

$$\begin{array}{c} \\ |1_h\rangle|0_k\rangle|0_l\rangle \\ |0_h\rangle|1_k\rangle|0_l\rangle \\ |0_h\rangle|0_k\rangle|1_l\rangle \end{array} \begin{array}{ccc} \langle 0_l|\langle 0_k|\langle 1_h| & \langle 0_l|\langle 1_k|\langle 0_h| & \langle 1_l|\langle 0_k|\langle 0_h| \\ \begin{pmatrix} 0 & 0 & 0 \\ -\dfrac{e^{i\left(\theta_2-\theta_1-\frac{\pi}{2}\right)}}{2\sqrt{2}} & \dfrac{e^{i(\theta_2-\theta_1-\theta_3)}}{4} & \dfrac{e^{i\left(\theta_2-\theta_1-\theta_3-\frac{\pi}{2}\right)}}{4} \\ \dfrac{e^{i(\theta_2-\theta_1)}}{2\sqrt{2}} & -\dfrac{e^{i\left(\theta_2-\theta_1-\theta_3+\frac{\pi}{2}\right)}}{4} & -\dfrac{e^{i(\theta_2-\theta_1-\theta_3)}}{4} \end{pmatrix} \end{array}$$

eqn. 16

Before the act of measurement by Alice, the density matrix is eqn. 14 (along with eqn. 15 and eqn. 16) but we can get the result quickly by using eqn. 7; by analogy,

$$|\psi\rangle = a|1_h\rangle|0_k\rangle|0_l\rangle + b|0_h\rangle|1_k\rangle|0_l\rangle + c|0_h\rangle|0_k\rangle|1_l\rangle$$

eqn. 17

The density matrix is:

$$\rho_{hkl} = |\psi\rangle\langle\psi|$$

$$= \begin{array}{c} |1_h\rangle|0_k\rangle|0_l\rangle \\ |0_h\rangle|1_k\rangle|0_l\rangle \\ |0_h\rangle|0_k\rangle|1_l\rangle \end{array} \begin{array}{ccc} \langle 0_l|\langle 0_k|\langle 1_h| & \langle 0_l|\langle 1_k|\langle 0_h| & \langle 1_l|\langle 0_k|\langle 0_h| \\ \begin{pmatrix} a^2 & ab^* & ac^* \\ ba^* & b^2 & bc^* \\ ca^* & cb^* & c^2 \end{pmatrix} \end{array}$$

eqn. 18

The partial trace is taken,

$$\rho_k = Tr_{hl}\left(\rho_{hlk}\right) \ or \ \rho_l = Tr_{hk}\left(\rho_{hlk}\right) \quad \text{eqn. 19}$$

Which yields,

$$\rho_l = a^2|0\rangle\langle 0| + c^2|1\rangle\langle 1|$$
$$\rho_k = a^2|0\rangle\langle 0| + b^2|1\rangle\langle 1|$$

eqn. 20

And the same probabilities are calculated as eqn. 8 and eqn. 9 but with the explicit representation of

the vacuum state interleaving between the times a photon isn't present.

After measurement by Alice, she is traced out of the system from the upper path thus,

$$\rho_{kl} = Tr_h\left(\rho_{hkl}\right)$$
$$= \langle 0_h|\rho_{hkl}|0_h\rangle + \langle 1_h|\rho_{hkl}|1_h\rangle$$

eqn. 21

The steps are shown in the appendix 1. This yields the reduced density matrix:-

$$\Rightarrow \rho_{kl} = \begin{array}{c} |0_k\rangle|0_l\rangle \\ |1_k\rangle|0_l\rangle \\ |0_k\rangle|1_l\rangle \end{array} \begin{array}{ccc} \langle 0_l|\langle 0_k| & \langle 0_l|\langle 1_k| & \langle 1_l|\langle 0_k| \\ \begin{pmatrix} \dfrac{e^{i(2\theta_1+\pi)}}{2} & 0 & 0 \\ 0 & \dfrac{e^{i(2\theta_1+\theta_2+\theta_3)}}{4} & 0 \\ 0 & 0 & \dfrac{e^{i(2\theta_1+\theta_2+\theta_3+\pi)}}{4} \end{pmatrix} \end{array}$$

$$+ \begin{array}{c} |0_k\rangle|0_l\rangle \\ |1_k\rangle|0_l\rangle \\ |0_k\rangle|1_l\rangle \end{array} \begin{array}{ccc} \langle 0_l|\langle 0_k| & \langle 0_l|\langle 1_k| & \langle 1_l|\langle 0_k| \\ \begin{pmatrix} 0 & 0 & 0 \\ 0 & \dfrac{e^{i(\theta_1-\theta_2+\theta_3)}+e^{i(\theta_2-\theta_1-\theta_3)}}{4} & \dfrac{e^{i\left(\theta_2-\theta_1-\theta_3-\frac{\pi}{2}\right)}-e^{i\left(\theta_1-\theta_2+\theta_3-\frac{\pi}{2}\right)}}{4} \\ 0 & \dfrac{e^{i\left(\theta_1-\theta_2+\theta_3+\frac{\pi}{2}\right)}-e^{i\left(\theta_2-\theta_1-\theta_3+\frac{\pi}{2}\right)}}{4} & \dfrac{-e^{i(\theta_1-\theta_2+\theta_3)}+e^{i(\theta_2-\theta_1-\theta_3)}}{4} \end{pmatrix} \end{array}$$

eqn. 22

Appendix 2 shows the results for the partial trace to obtain ρ_l and ρ_k from ρ_{kl} and these yield the same results as earlier for the non-interference (Alice measures) case but with the explicit representation of the vacuum state in the mixed state output.

4. Discussion and conclusion

The sum of paths/sum of amplitudes proof given in earlier papers for the 1-photon system (figure 2) was criticised as being a necessary but <u>not</u> a necessary and sufficient proof for superluminality – that is in some putative communication scheme, we must have modulation but that doesn't automatically imply superluminality. The proof, some believe, gives the impression of a photon wavefunction moving through the apparatus and traversing each component in a time-like fashion. We beg to differ, as by eqn. 4 (eqn. 10 too) show the summation of the wavefunctions from the upper and lower legs *after* they have been through the final beamsplitter. The expectation values at Bob's detectors have a feed-through component from Alice's splitter and her influence collapses her wavefunction, which is summed at Bob *outside* the apparatus (figure 3).

Is it to be believed that the wave function propagating *through* the interferometer is really the issue? If Alice's measurement is near to the interferometer, it would just seem that her influence has to propagate through the

apparatus until the final beamsplitter. We argue that the interferometer is merely the device for the correct setup of the rays emanating from the source to: go to Alice and then to Bob with some component from Alice. An overall global phase in the wavefunctions (representing the causal delay transiting the apparatus) does not appear in the expectation values and has no effect on it.

The state vector approach with sub-systems (i.e. rather than just consider the amplitudes for one photon, $|1\rangle$ but outputs $\sum_{i=h,k,l} a_i |1\rangle_h |0\rangle_k |0\rangle_l$ etc.) fairs better and got nearer the truth – far away from the interferometer, what is relevant is her coherence or not on Bob's interference pattern. However the state vector approach suffered from the apparent "sleight-of-hand" of having to manually enter the decoherence terms (despite the experimental fact of decoherence[11]). As such that proof is somewhat artificial and "clunky".

The full density matrix analysis given in this note gracefully handles Alice's measurement by the reduced trace. The absolute temporal <u>sequence</u> is important:-

> Alice measures first (partial trace), Bob performs his partial trace for one of the outputs.

> Alice doesn't measure first, Bob measures for one (or both) of his outputs and observes interference.

<u>What is intriguing</u> is that the *static* density matrix description of the system applies far away from the interferometer (it just sets up the rays from the source) and has no time element (no propagator), only the sequence in which the operations are performed matters. This implies space-like communication and corresponds to the notion that wavefunction collapse is instantaneous or near instantaneous.

References

1. Bell, J.S., *On the Einstein-Podolsky-Rosen Paradox.* Physics Letters A, 1964. **1**: p. 195-200.

2. Bell, J.S., *Foundations of Quantum Mechanics.* New York: Academic, 1971. **171**.

3. Roger, A. Aspect P. Grangier G., *Experimental Realization of Einstein-Podolsky-Rosen-Bohm Gedankenexperiment: A New Violation of Bell's Inequalities.* Phys. Rev. Lett., 1982. **49**(91).

4. Zbinden H., Gisin N., *Testing the speed of 'spooky action at a distance'.* Nature, 2008. **454**.

5. Sheehan D. P. *Quantum Retrocausation III.* 2016. University of San Diego, C.A.: AIP.

6. Everett H., *Relative State Formulation of Quantum Mechanics.* Reviews of Modern Physics, 1957. **29**: p. 454-462.

7. Zurek, W.H., *Decoherence and the Transition from Quantum to Classical.* Los Alamos Science, 2002. **27**.

8. Hall, M.J.W., *Imprecise Measurements and Non-Locality in Quantum Mechanics.* Physics Letters A, 1987. **125**(2,3): p. 89,91.

9. Ghirardi, G. C.; Rimini, A.; Weber, T., *A General Argument against Superluminal Transmission through the Quantum Mechanical Measurement Process.* Lettere al Nuovo Cimento, 1980, 8th March. **27**(10): p. 293-298.

10. Ghirardi, G. C.; Rimini, A.; Weber, T., *Experiments of the EPR Type Involving CP-Violation do not allow Faster-than-Light Communications Between Distant Observers.* Europhys. Lett., 1988. **6**(2): p. 95-100.

11. Cornwall, R.O., *Superluminal Signalling by Path Entanglement.* 2015 (https://www.academia.edu/12881902/Disproof_of_the_No-communication_Theorem_by_Decoherence_Theory).

12. Cornwall R. O., *Disproof of the No-communication Theorem by Decoherence Theory.* 2015 (https://www.academia.edu/12881902/Disproof_of_the_No-communication_Theorem_by_Decoherence_Theory).

13. Cornwall R. O., *The misuse of the No-communication Theorem.* 2016 (https://www.academia.edu/29296558/The_misuse_of_the_No-communication_Theorem).

14. Cornwall, R.O., *A Mechanism for the effects of Relativity* 2014 (https://www.academia.edu/11587819/A_Mechanism_for_the_effects_of_Relativity).

15. Wikipedia. *Faster-than-light neutrino anomaly*. 2019; Available from: https://en.wikipedia.org/wiki/Faster-than-light_neutrino_anomaly.

16. Lett, Ryan T. Glasser; Ulrich Vogl; Paul D., *Stimulated generation of superluminal light pulses via four-wave mixing.* Arxiv preprint, 2018 (https://arxiv.org/abs/1204.0810).

17. Cornwall, R.O., *Secure Quantum Communication and Superluminal Signalling on the Bell Channel.* Infinite Energy, 2006. **69** (https://www.academia.edu/11587674/Secure_Quantum_Communication_and_Superluminal_Signalling_on_the_Bell_Channel http://vixra.org/abs/1311.0074).

18. Ralph, Hans-A Bachor; Timothy C., *A Guide to Experiments in Quantum Optics.* 2004: Wiley-VCH.

19. Zeilinger, A., *General properties of lossless beam splitters in interferometry.* Am. J. Phys., 1981. **49**(9).

20. Gerry, Christopher; Knight, Peter, *Introductory Quantum Optics.* 2004: CUP.

Appendix 1

$$\rho_{kl} = Tr_h\left(\rho_{hkl}\right) = \langle 0_h | \rho_{hkl} | 0_h \rangle + \langle 1_h | \rho_{hkl} | 1_h \rangle$$

$\Rightarrow$

$$\rho_{kl} = \begin{array}{c} |0_k\rangle|0_l\rangle \\ |1_k\rangle|0_l\rangle \\ |0_k\rangle|1_l\rangle \end{array}
\begin{pmatrix}
\dfrac{e^{i(2\theta_1+\pi)}}{2} & 0 & 0 \\[2mm]
0 & \dfrac{e^{i2(\theta_1+\theta_3)}}{4} & \dfrac{e^{-i\frac{\pi}{2}}}{4} \\[2mm]
0 & \dfrac{e^{i\frac{\pi}{2}}}{4} & \dfrac{e^{i(2\theta_1+2\theta_3+\pi)}}{4}
\end{pmatrix}$$

with columns $\langle 0_l|\langle 0_k|$, $\langle 0_l|\langle 1_k|$, $\langle 1_l|\langle 0_k|$

$$+ \begin{array}{c} |0_k\rangle|0_l\rangle \\ |1_k\rangle|0_l\rangle \\ |0_k\rangle|1_l\rangle \end{array}
\begin{pmatrix}
0 & 0 & 0 \\[2mm]
0 & \dfrac{e^{i2\theta_2}}{4} & -\dfrac{e^{-i\frac{\pi}{2}}}{4} \\[2mm]
0 & -\dfrac{e^{i\frac{\pi}{2}}}{4} & \dfrac{e^{i2\theta_2+\pi}}{4}
\end{pmatrix}$$

columns $\langle 0_l|\langle 0_k|$, $\langle 0_l|\langle 1_k|$, $\langle 1_l|\langle 0_k|$

$$+ \begin{array}{c} |0_k\rangle|0_l\rangle \\ |1_k\rangle|0_l\rangle \\ |0_k\rangle|1_l\rangle \end{array}
\begin{pmatrix}
0 & 0 & 0 \\[2mm]
0 & \dfrac{e^{i(\theta_1-\theta_2+\theta_3)}}{4} & -\dfrac{e^{i\left(\theta_1-\theta_2+\theta_3-\frac{\pi}{2}\right)}}{4} \\[2mm]
0 & \dfrac{e^{i\left(\theta_1-\theta_2+\theta_3+\frac{\pi}{2}\right)}}{4} & -\dfrac{e^{i(\theta_1-\theta_2+\theta_3)}}{4}
\end{pmatrix}$$

columns $\langle 0_l|\langle 0_k|$, $\langle 0_l|\langle 1_k|$, $\langle 1_l|\langle 0_k|$

$$+ \begin{array}{c} |0_k\rangle|0_l\rangle \\ |1_k\rangle|0_l\rangle \\ |0_k\rangle|1_l\rangle \end{array}
\begin{pmatrix}
0 & 0 & 0 \\[2mm]
0 & \dfrac{e^{i(\theta_2-\theta_1-\theta_3)}}{4} & \dfrac{e^{i\left(\theta_2-\theta_1-\theta_3-\frac{\pi}{2}\right)}}{4} \\[2mm]
0 & -\dfrac{e^{i\left(\theta_2-\theta_1-\theta_3+\frac{\pi}{2}\right)}}{4} & -\dfrac{e^{i(\theta_2-\theta_1-\theta_3)}}{4}
\end{pmatrix}$$

columns $\langle 0_l|\langle 0_k|$, $\langle 0_l|\langle 1_k|$, $\langle 1_l|\langle 0_k|$

$$\Rightarrow \rho_{kl} = \begin{array}{c} |0_k\rangle|0_l\rangle \\ |1_k\rangle|0_l\rangle \\ |0_k\rangle|1_l\rangle \end{array}
\begin{pmatrix}
\dfrac{e^{i(2\theta_1+\pi)}}{2} & 0 & 0 \\[2mm]
0 & \dfrac{e^{i2(\theta_1+\theta_2+\theta_3)}}{4} & 0 \\[2mm]
0 & 0 & \dfrac{e^{i2(\theta_1+\theta_2+\theta_3+\pi)}}{4}
\end{pmatrix}$$

columns $\langle 0_l|\langle 0_k|$, $\langle 0_l|\langle 1_k|$, $\langle 1_l|\langle 0_k|$

$$+ \begin{array}{c} |0_k\rangle|0_l\rangle \\ |1_k\rangle|0_l\rangle \\ |0_k\rangle|1_l\rangle \end{array}
\begin{pmatrix}
0 & 0 & 0 \\[2mm]
0 & \dfrac{e^{i(\theta_1-\theta_2+\theta_3)}+e^{i(\theta_2-\theta_1-\theta_3)}}{4} & \dfrac{e^{i\left(\theta_2-\theta_1-\theta_3-\frac{\pi}{2}\right)}-e^{i\left(\theta_1-\theta_2+\theta_3-\frac{\pi}{2}\right)}}{4} \\[2mm]
0 & \dfrac{e^{i\left(\theta_1-\theta_2+\theta_3+\frac{\pi}{2}\right)}-e^{i\left(\theta_2-\theta_1-\theta_3+\frac{\pi}{2}\right)}}{4} & -\dfrac{e^{i(\theta_1-\theta_2+\theta_3)}+e^{i(\theta_2-\theta_1-\theta_3)}}{4}
\end{pmatrix}$$

columns $\langle 0_l|\langle 0_k|$, $\langle 0_l|\langle 1_k|$, $\langle 1_l|\langle 0_k|$

Appendix 2

$$\rho_k = Tr_l\left(\rho_{kl}\right) = \langle 0_l | \rho_{kl} | 0_l \rangle + \langle 1_l | \rho_{kl} | 1_l \rangle$$

$\Rightarrow$

$$\rho_k = \begin{array}{c} |0_k\rangle \\ |1_k\rangle \end{array}
\begin{pmatrix}
\dfrac{e^{i(2\theta_1+\pi)}}{2}+\dfrac{e^{i2(\theta_1+\theta_2+\theta_3+\pi)}}{4} & 0 \\[2mm]
0 & \dfrac{e^{i2(\theta_1+\theta_2+\theta_3)}}{4}
\end{pmatrix}$$

columns $\langle 0_k|$, $\langle 1_k|$

$$+ \begin{array}{c} |0_k\rangle \\ |1_k\rangle \end{array}
\begin{pmatrix}
-\dfrac{e^{i(\theta_1-\theta_2+\theta_3)}+e^{i(\theta_2-\theta_1-\theta_3)}}{4} & 0 \\[2mm]
0 & \dfrac{e^{i(\theta_1-\theta_2+\theta_3)}+e^{i(\theta_2-\theta_1-\theta_3)}}{4}
\end{pmatrix}$$

columns $\langle 0_k|$, $\langle 1_k|$

Appendix 2 (cont)

$$\rho_l = Tr_k\left(\rho_{kl}\right)$$
$$= \left\langle 0_k \left| \rho_{kl} \right| 0_k \right\rangle + \left\langle 1_k \left| \rho_{kl} \right| 1_k \right\rangle$$

$\Rightarrow$

$$\rho_l = \begin{array}{c} \\ |0_l\rangle \\ \\ |1_l\rangle \end{array} \begin{array}{cc} \langle 0_l| & \langle 1_l| \\ \left[\dfrac{e^{i(2\theta_1+\pi)}}{2} + \dfrac{e^{i2(\theta_1+\theta_2+\theta_3+\pi)}}{4} & 0 \\ 0 & \dfrac{e^{i2(\theta_1+\theta_2+\theta_3)}}{4} \end{array} \right]$$

$$+ \begin{array}{c} \\ |0_l\rangle \\ \\ |1_l\rangle \end{array} \begin{array}{cc} \langle 0_l| & \langle 1_l| \\ \left[-\dfrac{e^{i(\theta_1-\theta_2+\theta_3)} + e^{i(\theta_2-\theta_1-\theta_3)}}{4} & 0 \\ 0 & \dfrac{e^{i(\theta_1-\theta_2+\theta_3)} + e^{i(\theta_2-\theta_1-\theta_3)}}{4} \end{array} \right]$$